

## TRANSFER OF CHARGE IN A PARTICULATE IRON-ELECTROLYTE SYSTEM

Miroslav F. GÁL<sup>1</sup>, Miriam GÁLOVÁ<sup>2,\*</sup> and Andrea TUROŇOVÁ<sup>3</sup>

Faculty of Science, P. J. Šafárik University, Moyzesova 11, 04154 Košice, Slovak Republic;  
e-mail: <sup>1</sup> mirgal@kosice.upjs.sk, <sup>2</sup> mgalova@kosice.upjs.sk, <sup>3</sup> aturon@kosice.upjs.sk

Received April 17, 2000  
Accepted August 15, 2000

*Dedicated to Professor Ludovít Treindl on the occasion of his 70th birthday.*

Mechanism of the charge transfer through a heterogeneous system consisting of Fe powder particles suspended in nickel-plating electrolyte was studied in the regime of electrolysis. Conductivity and impedance spectra were used to elucidate the contribution of solid particles to the charge transfer through the cell. Combined short-circuit and collision mechanism takes place in low-density suspensions. A complete elucidation of the mechanism is complicated by the presence of powder particles of three groups: particles carrying the charge, uncharged particles representing just a barrier to the charge transfer and particles passivated during the electrolysis by adsorption of an isolating layer of Fe and Ni hydroxocomplexes. The formation of powder aggregates in high-density suspensions was indirectly evidenced.

**Key words:** Electrolysis; Powder particles; Fluidized bed; Conductance; Impedance spectra; Iron; Nickel.

Various mechanisms of charge transfer in electrolyte solutions of very low, moderate, and very high concentrations of ionic species have been well known for many years. The situation is different in a heterogeneous system consisting of conducting powder particles suspended in an electrolyte. This is the case of "fluidized bed electrodes" where powder particles are kept in suspension either by vertical electrolyte flow or by circular stirring. Such arrangement, first published in 1966 (refs<sup>1,2</sup>), was designed to increase the surface to volume ratio of the active electrode. Its practical importance was tested in electroorganic synthesis<sup>3</sup>, metal recovery<sup>4,5</sup>, and fuel cell development<sup>6</sup>. In our laboratory, metal plating of powder particles was studied with the aim to employ such material in powder metallurgy after proper processing<sup>7,8</sup>.

The charge transport through the bed may be realized both by the electrolyte and by solid particles depending on their conductivity: less conduct-

ing particles act rather as an insulator while well conductive metallic particles would contribute more or less to the total conductivity of the system<sup>9</sup>. In such a case, an important factor is the concentration of solid particles in the bed, or, the density of suspension. For the fluidized bed, this quantity can be expressed as "voidage  $\varepsilon$ " defined by Eq. (1) (ref.<sup>9</sup>):

$$\varepsilon = \frac{V_e}{V_e + V_s}, \quad (1)$$

where  $V_e$  is the electrolyte volume and  $V_s$  the volume of the solid phase.

The voidage is to a great extent responsible for the mechanism of charge transfer through a fluidized bed. Charge may pass through the system either by the contact of ions or particles with the solid electrode and with each other or by bipolar charged particles existing in the electric field. An isolated particle immersed in an electrolyte having an imposed potential gradient will support anodic and cathodic reactions on opposite faces provided the ohmic resistance of the particle is lower than that of the surrounding electrolyte. The current may be transferred between the phases by a surface redox reaction, the resistance of which is determined by the rate of the electrochemical process<sup>10</sup>. This idea was further developed by a bipolar analysis of a single sphere in an electrolytic cell<sup>11</sup>. Thus, the most frequent mechanisms may be classified as follows: (i) simple ionic conductance, (ii) short circuit combined ionic and electronic conductance<sup>12</sup>, (iii) collision (convective) mechanism<sup>13</sup>, (iv) conductive (electronic) mechanism<sup>12,14</sup>.

Simple ionic conductance is realized in beds with non-conducting solid particles. Short circuit conductance means that the charge passes in addition to ionic conductance also by the electron conductivity of solid particles. Generally, the most accepted and best developed in many details is the convective mechanism<sup>13</sup>. The charge is transported by collisions of particles with the working electrode and further by their mutual collisions in the fluidized bed suspension. However, exact calculations show that the number of collisions required to the complete charge transfer is enormously high. The theory was expanded by the idea of collisions of aggregates of particles<sup>15</sup>. Measurements of the effective conductance of the bed *vs* AC frequency<sup>12,16</sup> resulted to an alternative electronic mechanism where the charge transfer through chains or aggregated particles in contact with the working electrode was assumed. The life-time of such chains and aggregates is rather short, their disintegration and new formation cause fluctuation and local overvoltage in the bed. The concept of bipolar chains and

aggregates in the bulk of the bed was introduced<sup>14</sup> in order to explain some of these effects. Obviously, the probability of such phenomena drops with increasing bed expansion, as exactly calculated<sup>14</sup>. An important contribution to the elucidation of effects in the fluidized bed are impedance measurements<sup>17</sup>.

In the present work, the mechanism of charge transfer was investigated in a bed consisting of Fe powder particles in a nickel sulfate acidic electrolyte. Here, the electrolytic nickel plating of powder particles took place. The influence of suspension density, particle size, and current intensity was studied by conductivity measurements during galvanostatic electrolysis and by measuring the impedance spectra at various frequencies.

## EXPERIMENTAL

### Materials

Fe powder was sieved into five fractions: 0–45, 45–63, 63–100, 100–125, 125–160  $\mu\text{m}$ . Prior to electrolysis, the powder was activated chemically by reduction in a 10% hydrazinium hydrochloride solution for 3–5 min, washed with distilled water and methanol or acetone, and dried.

The composition of the nickel plating electrolyte used for conductometric measurements was as follows: 1.2 M  $\text{NiSO}_4$ , 0.6 M NaCl, 0.6 M  $\text{H}_3\text{BO}_3$ . For impedance measurements, 0.6 M  $\text{NiSO}_4$  was employed as electrolyte.

The powder was kept in suspension by stirring at 450 rpm for conductance measurements and 210 rpm for impedance measurements.

### Apparatus and Equipment

The conductance measurements were carried out using a conductometer K912 (Consort) equipped with a four-electrode flow cell S612T (Consort) designed for experiments in suspensions. Galvanostatic electrolyses were performed in a cell described in Fig. 1. The conductance cell was introduced into the cathodic compartment of the electrolyser. A stainless

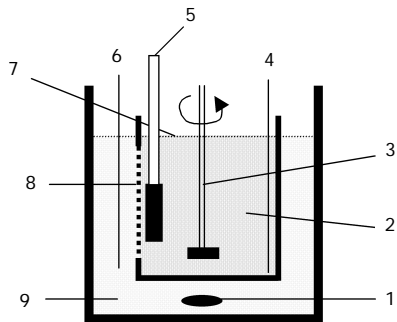


FIG. 1

Schematic representation of the fluidized bed cell: 1 magnetic stirrer, 2 cathodic compartment, 3 mechanical stirrer, 4 stainless steel cathode, 5 conductance cell, 6 counter electrode, 7 electrolyte level, 8 diaphragm, 9 anodic compartment

steel sheet of  $21.75 \text{ cm}^2$  surface area acted as a cathode. The anode was made of pure nickel. Cathodic and anodic compartments were separated by a textile net diaphragm with pores diameter of 0.004 mm to prevent passing of powder particles into the anodic part.

Acrylic glass cell for impedance measurements, designed in our laboratory, is shown in Fig. 2. Both cathode and anode were made of pure copper. The surface area of the cathode was  $5 \text{ mm}^2$  and that of the anode  $400 \text{ mm}^2$ . As it can be seen from the Fig. 2, the cell construction prevented the powder particles transfer from the cathodic into the anodic compartment. Measurements were made using a laboratory-built electrochemical system<sup>18</sup> consisting of a fast rise-time potentiostat interfaced to a personal computer via the IEEE-interface card PCLab model 748 (AdvanTech Co, U.S.A.). The voltage source was either a 12-bit D/A card PCLab model 818 or a programmable arbitrary-function generator Stanford Research model DS340. The impedance measurements were performed in the range of 1 Hz–100 kHz using a network analyzer Stanford Research model SR780. The AC voltage of 5 mV amplitude was derived from an internal oscillator of the network analyzer. A three-electrode electrochemical system was used with an Ag/AgCl in 1 M LiCl reference electrode separated from the test solution by a salt bridge.

## RESULTS AND DISCUSSION

### Conductivity Measurements

The conductivity of Fe powder suspension in given electrolyte was measured at stepwise increasing suspension density. Curve 1 in Fig. 3 proves that powder particles, despite of conductive character represent only a mechanical barrier to the ionic transport of the charge. The situation is different if the regime of galvanostatic electrolysis is applied (see curve 2). If current is passing through the cell, the conductivity of the suspension increases and is higher in the whole range of the suspension density as compared to values aquired without electrolysis. Curve 3 shows the course of

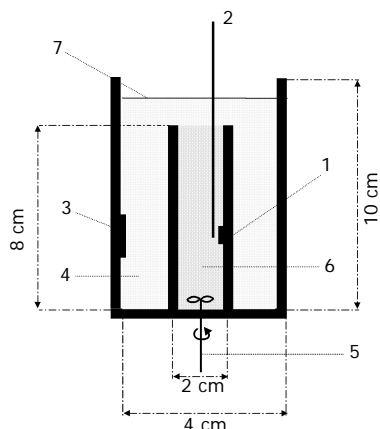


FIG. 2

Scheme of the cell for impedance measurements: 1 working electrode, 2 reference electrode, 3 counter electrode, 4 anodic compartment, 5 mechanical stirrer, 6 cathodic compartment, 7 electrolyte level

conductivity upon the electrolysis of a suspension of non-conducting  $\text{Al}_2\text{O}_3$  particles. The decrease in conductivity to a higher extent than with conducting Fe particles without electrolysis is observed.

This may be ascribed to the contribution of charged solid particles to the conductivity. The Fe powder particles acquire a charge during their contacts with the solid cathode whereas non-conductive  $\text{Al}_2\text{O}_3$  particles unable to acquire any charge from the solid electrode decrease the conductivity. Although it may seem unlikely at such high values of voidage, the high specific weight of Fe should be taken into account and the experimental results are evident. In addition to curve 3 in Fig. 3 measured with electrolysis another experiments were carried out to exclude the influence of electrolyte composition changes during electrolysis which may change conductivity. Changes of conductivity in both low and high suspension density systems during 60 min electrolysis were observed. Upon an addition of 5 g of Fe powder (size fraction 63–100  $\mu\text{m}$ ) to 150 ml of catholyte, which corresponds to the maximum on curve 2 in Fig. 3, the conductivity values oscillate at  $79 \pm 1.8 \text{ mS cm}^{-1}$ . Upon an addition of 50 g of Fe powder corresponding to the descending part of the same curve, the values oscillate between  $65 \pm 2.1 \text{ mS cm}^{-1}$  (see Fig. 4).

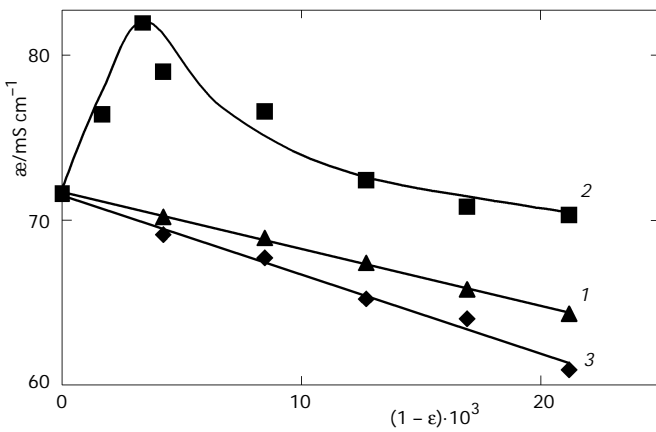


FIG. 3  
Change of conductivity with the suspension density for Fe or  $\text{Al}_2\text{O}_3$  suspensions in the electrolyte with and without electrolysis (particle size fraction 63–100  $\mu\text{m}$ , electrolysis current 1 A): 1 suspension of Fe powder particles without electrolysis, 2 suspension of Fe powder particles with electrolysis applied, 3 suspension of  $\text{Al}_2\text{O}_3$  powder particles with electrolysis applied

Further experimental results supporting the idea of contribution of charged particles to the conductivity values are presented in Fig. 4. It summarizes the effect of charged particles on the conductivity in the whole range of suspension densities and particle sizes investigated during the galvanostatic electrolysis. The first and second additions of Fe powder to the electrolyte cause the conductivity to increase to a maximum placed rather at low suspension density. The increase in conductivity is the highest for the smallest particle size fraction and gradually drops with the increasing particle size. Relative increments of conductivity increase in the maximum referred to the same suspension density without electrolysis are listed for various currents in Table I. For the minimum particle size, the conductivity increases by 19% at 1 A and by 42% at 3 A of electrolytic current compared to a "non-electrolytic" regime.

Differences in conductivity for various particle size fractions seem to support the idea that at low suspension density collisions of particles with the electrode as well as mutual collisions of particles take part in the charge transfer in the system. In a suspension of small particles, more particles are present in a volume unit and thus, the collision probability is higher. Calculations carried out according to an earlier developed model<sup>19</sup> show that at the same suspension density, the number of smallest particles is several times higher than that of largest particles, as shown in Table II. Experimental results also prove that under given conditions the increase in

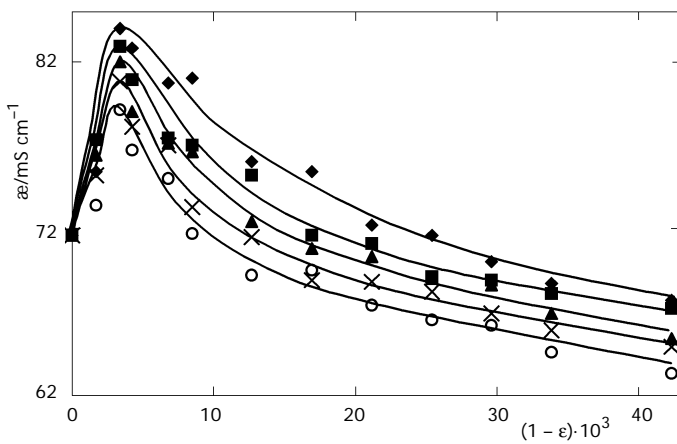


FIG. 4  
Change in conductivity with the suspension density and particle size fraction with electrolysis applied (electrolysis current 1 A). Particle size fraction (in  $\mu\text{m}$ ):  $\blacklozenge$  0-45,  $\blacksquare$  45-63,  $\blacktriangle$  63-100,  $\times$  100-125,  $\circ$  125-160

TABLE I

Increase of conductivity  $f_G$  for suspension of Fe powder of various size in Ni electrolyte in galvanostatic electrolysis at the maximum of curves in Fig. 2 relative to the conductivity in the same system without electrolysis

Current, A	$f_G$				
	0–45 $\mu\text{m}$	45–63 $\mu\text{m}$	63–100 $\mu\text{m}$	100–125 $\mu\text{m}$	125–160 $\mu\text{m}$
1	1.191	1.177	1.163	1.146	1.119
2	1.337	1.307	1.283	1.250	1.237
3	1.421	1.383	1.367	1.325	1.288

TABLE II

The number of particles in  $1 \text{ cm}^3$  in the impedance cell calculated according to the model<sup>19</sup> for various suspension densities and the smallest and largest particle size fractions

Suspension density $(1 - \varepsilon) \cdot 10^3$	The number of particles in $1 \text{ cm}^3$	
	45–63 $\mu\text{m}$	125–160 $\mu\text{m}$
1.6	24 962	–
2.6	–	2 206
3.0	47 845	–
6.5	102 341	5 557
12.1	–	10 459
18.0	277 010	–
27.6	–	24 152
30.3	490 573	–
43.0	–	38 240
60.3	1 003 682	–
85.6	–	79 851
109.5	1 925 641	–
179.0	–	185 461

conductivity cannot be explained only by the short circuit between solid particles in contact<sup>20</sup>. In such a case the conductivity of the coarse suspension would be higher than that of the fine one. Thus, the combination of both effects with prevailing collision mechanism would be the most probable explanation in addition to the ionic conductance model.

The decreasing course of curves after passing their maximum (Fig. 4) is assigned to increasing number of uncharged particles in the bed creating a barrier to the charge transfer. This assumption is supported by the impedance spectra (see the  $R_s$  values in Fig. 9). Moreover, at higher suspension densities the Fe powder particles become less conducting due to formation of a passivating layer on their surface. The latter assumption was verified by the measurement of polarization curves during Ni-plating of Fe powder particles (Fig. 5). A decrease in current on the cathodic side of the curve at a potentials around -0.9 and -1.1 V was explained as follows: Due to hydrogen evolution from the acidic electrolyte and, consequently, increase of pH in the vicinity of the electrode, insoluble hydroxo complexes of Fe and Ni are formed. They are adsorbed on the surface of powder particles (which act as a part of the electrode) and inhibit the electrode process. These measurements were completed by determination of the amount of Fe(II) ions dissolved from the powder as well as by analysis of the layer adsorbed on the powder surface<sup>21</sup>. Both experiments evidenced the fact that with increasing

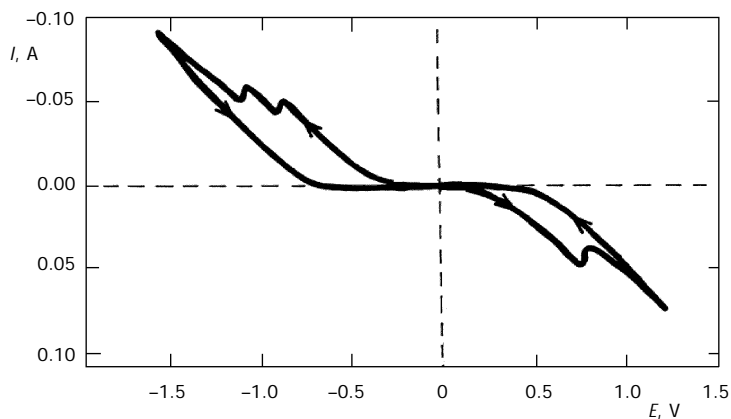


FIG. 5  
Current-potential curve for Ni electrolytic coating of Fe powder particles. Suspension density  $(1 - \varepsilon) \cdot 10^3 = 8.39$ , particle size fraction 63–100  $\mu\text{m}$ , rotation speed 200 rpm; working electrode: paraffin-impregnated graphite, counter electrode: Pt sheet, reference electrode: Ag/AgCl

amount of powder in the suspension, *i.e.* with increasing the suspension density both the amount of iron ions in solution and of adsorbed compounds on the powder surface increase. The conductivity decrease after the maximum, seen in Fig. 4, may thus also be ascribed to the formation of a passivation layer on the surface of powder particles.

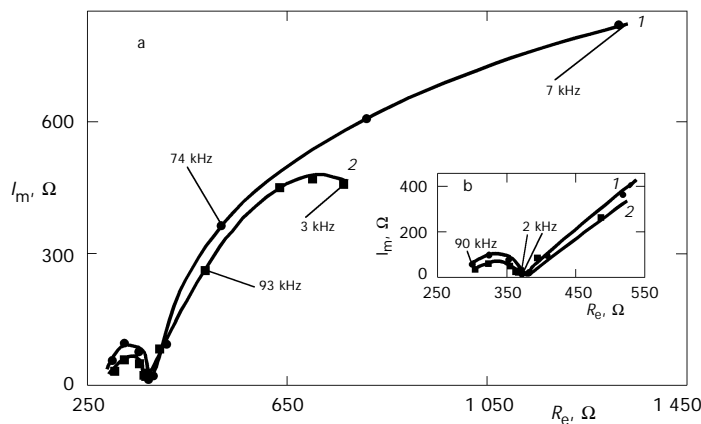


FIG. 6

Impedance spectra measured at various suspension densities: a wide frequency range, b narrow frequency range. Potentiostatic regime, potential of the working electrode -600 mV, particle size fraction 125–160  $\mu\text{m}$ , frequencies in Hz. Suspension density  $(1 - \varepsilon) \cdot 10^3$ : 1 27.6, 2 43

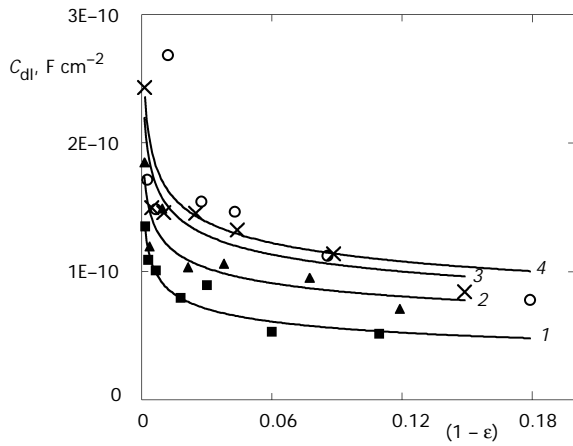


FIG. 7

Change of the particles double-layer capacity  $C_{dl}$  values with the suspension density. Particle size fraction (in  $\mu\text{m}$ ): 1 45–63, 2 63–100, 3 100–125, 4 125–160

### Impedance Measurements

Typical impedance spectra at higher and lower suspension densities are shown in Fig. 6. From measurements in the whole range of suspension densities and particle size fractions, capacities of the double layer, charge transfer resistances, and ohmic resistances of the suspension were calculated.

The dependence of the double-layer capacity ( $C_{dl}$ ) on the suspension density is shown in Fig. 7 for various particle size fractions. The suspension

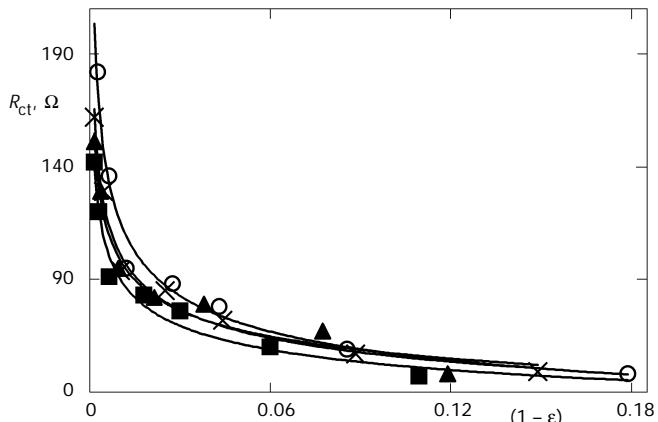


FIG. 8

Charge-transfer resistance  $R_{ct}$  as a dependence of suspension density. Particle size fraction (in  $\mu\text{m}$ ): ■ 45-63, ▲ 63-100, × 100-125, ○ 125-160

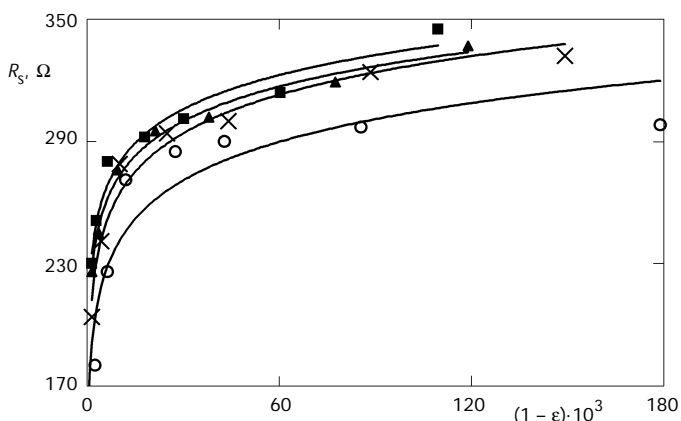


FIG. 9

Change of the ohmic suspension resistance  $R_s$  values with suspension density. Particle size fraction (in  $\mu\text{m}$ ): ■ 45-63, ▲ 63-100, × 100-125, ○ 125-160

density seems to influence  $C_{dl}$  only at very low values in accordance with the above statement on collision charge transfer mechanism in the low suspension density region. Here, the double-layer capacity of particles is a decisive factor in carrying the charge from the cathode to the solution and transferring it to other solid particles. The  $C_{dl}/S$  values show a tendency to decrease with decreasing particle size, however, these results may not be wholly reliable since the powder surface area  $S$  calculated at high suspension density according to the model<sup>8,19</sup> may not correspond to the actual surface area owing to chains and aggregates formation. By the way, the use of linear dimension of particles for calculating their specific surface area in the given fraction corresponds very well to declared surfaces and reflects adequately differences between fractions.

The charge-transfer resistance values  $R_{ct}$  shown in Fig. 8 are fairly independent of the particle size. Remarkable changes in  $R_{ct}$  values are observed only at low suspension densities. It would indicate that the rate of the electrode reaction increases in this region with increasing suspension density.

The ohmic resistance of the suspension  $R_s$  is shown in Fig. 9 in dependence on the suspension density. Evidently, the largest contribution to this quantity is made by uncharged solid particles. By the comparison of the number of particles in the lowest and highest particle size fractions (Table II) it is evident that the number of uncharged particles is much higher in low size fractions and, consequently, the ohmic resistance of such suspension is also higher.

The authors are indebted to Dr L. Pospíšil (J. Heyrovský Institute of Physical Chemistry, Academy of Sciences of the Czech Republic, Prague) for providing the experimental equipment as well as for valuable consultations in the field of impedance measurements. Thanks should be also given to Dr L. Lux (Technical University, Košice, Slovak Republic) for valuable discussions. Financial support from the Grant Agency of the Slovak Republic (Project No. 1/6024/99) is gratefully acknowledged.

## REFERENCES

1. Coeuret F., Le Golf P., Vergnes F.: Fr. 1500269, 1967.
2. Backhurst J. R., Fleischmann M., Goodridge P., Plimley R. E.: Brit. 1194181, 1970.
3. Enriquez-Granados M. A., Hutin D., Storck A.: *Electrochim. Acta* **1982**, *27*, 303.
4. Coeuret F.: *J. Appl. Electrochem.* **1980**, *10*, 687.
5. Van der Heiden G., Raats M. S., Boon H. F.: *Chem. Ind. (London)* **1978**, 465.
6. Le Golf P., Vergnes F., Coeuret F., Bordet J.: *Ind. Eng. Chem.* **1969**, *91*, 8.
7. Lux L., Gálová M., Oriňáková R., Turoňová A.: *Particulate Sci. Technol.* **1998**, *16*, 135.
8. Gálová M., Oriňáková R., Lux L.: *J. Solid State Electrochem.* **1998**, *2*, 2.
9. Roušar I., Micka K., Kimla A.: *Electrochemical Engineering* 2, p. 213. Academia, Prague 1986.

10. Eardley D. C., Handley D., Andrew S. P. S.: *Electrochim. Acta* **1973**, *18*, 839.
11. Yen S. Ch., Yao Ch. Y.: *J. Electrochem. Soc.* **1991**, *138*, 2697.
12. Sabacky B. J., Evans J. W.: *Metall. Mater. Trans. B* **1977**, *8*, 5.
13. Fleischmann M., Oldfield J. W.: *J. Electroanal. Chem. Interfacial Electrochem.* **1971**, *29*, 231.
14. Plimley R. E., Wright A. R.: *Chem. Eng. Sci.* **1984**, *39*, 395.
15. Beenackers A. A., van Swaaij W. P., Welmers A.: *Electrochim. Acta* **1977**, *22*, 1277.
16. Sabacky B. J., Evans J. W.: *J. Electrochem. Soc.* **1979**, *126*, 1176.
17. a) Gabrielli C., Huet F., Sarah A., Valentin G.: *J. Appl. Electrochem.* **1992**, *22*, 801; b) Huh T., Evans J. W.: *J. Electrochem. Soc.* **1987**, *134*, 308; c) Huh T., Evans J. W.: *J. Electrochem. Soc.* **1987**, *134*, 317; d) Gabrielli C., Huet F., Sarah A., Valentin G.: *J. Appl. Electrochem.* **1994**, *24*, 481.
18. Pospíšil L., Fiedler J., Fanelli N.: *Rev. Sci. Instrum.* **2000**, *71*, 1804.
19. Lux L., Stašková R., Gálová M.: *Acta Chim. – Models in Chemistry* **1996**, *133*, 115.
20. Yen S. Ch., Yao Ch. Y.: *J. Electrochem. Soc.* **1991**, *138*, 2697.
21. Turoňová A., Gálová M.: *Trans. Univ. Kosice* **1999**, *1*, 47.